

## Experimental investigations of the hypernucleus ${}^4_{\Lambda}\text{H}$

P. Achenbach<sup>1,a</sup>, F. Schulz<sup>1,b</sup>, S. Aulenbacher<sup>1</sup>, J. Beričič<sup>2</sup>, S. Bleser<sup>1,3</sup>, R. Böhm<sup>1</sup>, D. Bosnar<sup>4</sup>, L. Correa<sup>5</sup>, M. O. Distler<sup>1</sup>, A. Esser<sup>1</sup>, H. Fonvieille<sup>5</sup>, I. Friščič<sup>4</sup>, Y. Fujii<sup>6</sup>, M. Fujita<sup>6</sup>, T. Gogami<sup>6,c</sup>, H. Kanda<sup>6</sup>, M. Kaneta<sup>6</sup>, S. Kegel<sup>1</sup>, Y. Kohl<sup>1</sup>, W. Kusaka<sup>6</sup>, A. Margaryan<sup>7</sup>, H. Merkel<sup>1</sup>, M. Mihovilović<sup>1</sup>, U. Müller<sup>1</sup>, S. Nagao<sup>6</sup>, S. N. Nakamura<sup>6</sup>, J. Pochodzalla<sup>1</sup>, A. Sanchez Lorente<sup>1,3</sup>, B. S. Schlimme<sup>1</sup>, M. Schoth<sup>1</sup>, C. Sfienti<sup>1</sup>, S. Širca<sup>2</sup>, M. Steinen<sup>1,3</sup>, Y. Takahashi<sup>6</sup>, L. Tang<sup>8</sup>, M. Thiel<sup>1</sup>, K. Tsukada<sup>6,d</sup>, A. Tyukin<sup>1</sup>, and A. Weber<sup>1</sup>

(A1 Collaboration)

<sup>1</sup>*Institut für Kernphysik, Johannes Gutenberg-Universität, D-55099 Mainz, Germany*

<sup>2</sup>*Department of Physics, University of Ljubljana, and Jožef Stefan Institute, SI-1000 Ljubljana, Slovenia*

<sup>3</sup>*Helmholtz Institute Mainz, D-55099 Mainz, Germany*

<sup>4</sup>*Department of Physics, University of Zagreb, HR-10002 Zagreb, Croatia*

<sup>5</sup>*LPC-Clermont, Université Blaise Pascal, CNRS/IN2P3, F-63177 Aubière Cedex, France*

<sup>6</sup>*Department of Physics, Tohoku University, Sendai, 980-8571, Japan*

<sup>7</sup>*Yerevan Physics Institute, 375036 Yerevan, Armenia*

<sup>8</sup>*Department of Physics, Hampton University, Hampton, Virginia 23668, USA*

**Abstract.** Negatively charged pions from two-body decays of stopped  ${}^4_{\Lambda}\text{H}$  hypernuclei were studied in 2012 at the Mainz Microtron MAMI, Germany. The momenta of the decay-pions were measured with unprecedented precision by using high-resolution magnetic spectrometers. A challenge of the experiment was the tagging of kaons from associated  $K^+\Lambda$  production off a Be target at very forward angles. In the year 2014, this experiment was continued with a better control of the systematic uncertainties, with better suppression of coincident and random background, improved particle identification, and with higher luminosities. Another key point of the progress was the improvement in the absolute momentum calibration of the magnetic spectrometers.

## 1 Introduction

The structure of light  $\Lambda$ -hypernuclei and the precise determination of  $\Lambda$  binding (separation) energies has been the focus of recent experimental and theoretical programs. The  $\Lambda$ -hypernucleus  ${}^4_{\Lambda}\text{H}$  was investigated in 2012 by high-resolution spectroscopy at the Mainz Microtron MAMI, Germany [1]. In this experiment the binding energy of  ${}^4_{\Lambda}\text{H}$  was determined from the two-body charged decay mode with an unprecedented  $\pm 10$  keV statistical uncertainty and  $\pm 90$  keV systematic uncertainty to be  $B_{\Lambda} =$

<sup>a</sup>e-mail: patrick@kph.uni-mainz.de

<sup>b</sup>Part of doctoral thesis.

<sup>c</sup>Present address: Graduate School of Science, Kyoto University, Kyoto 606-8502, Japan.

<sup>d</sup>Present address: Research Center for Electron Photon Science, Tohoku University, Sendai 982-0826, Japan.

2.12 MeV. This value is 80 keV different from emulsion data, the most complete compilation of which found  $B_{\Lambda} = 2.04 \pm 0.04$  MeV using only three-body charged decay modes [2].

The new method of decay-pion spectroscopy has the potential to allow binding energy measurements of several light hypernuclei with a precision comparable or better than with the emulsion technique. The statistical uncertainty for the binding energies in light hypernuclei with the emulsion method ranged from a minimum of 20 keV for the most abundant hypernuclei  ${}^5_{\Lambda}\text{He}$  to more than 700 keV for  ${}^8_{\Lambda}\text{He}$  [2–4]. Systematic errors in the emulsion data are not shown, but D.H. Davis assumed errors of the order of 50 keV [5].

A major effort in hypernuclear physics is to understand the interaction between hyperons and nucleons. One motivation to study the  ${}^4_{\Lambda}\text{H}$  hypernucleus is the possible difference between the hyperon–proton and hyperon–neutron interaction which is manifest in the difference of  $\Lambda$  binding energies,  $\Delta B_{\Lambda}^4$ , in the mirror pair of hypernuclei  ${}^4_{\Lambda}\text{H}$  and  ${}^4_{\Lambda}\text{He}$ . This difference of  $\Delta B_{\Lambda}^4 = 350 \pm 60$  (stat.) keV is one of the main sources of information about the charge symmetry breaking (CSB) in the  $\Lambda N$  interaction, see Ref. [6] for a recent review. The improvement of the uncertainties on the binding energy of  ${}^4_{\Lambda}\text{He}$  is outside the potentialities of decay-pion spectroscopy because this hypernucleus cannot decay in the two-body pionic channel. Combined with the emulsion data of  $B_{\Lambda}({}^4_{\Lambda}\text{He})$ , the MAMI experiment indicates a large  $\Delta B_{\Lambda}^4$ . This supports a CSB effect in the  $\Lambda N$  interaction being much larger than in the  $NN$  interaction.

In the year 2014 the MAMI experiment was continued. In this paper, the control of systematic uncertainties, the improvements in background suppression, and the extensive calibrations are discussed which reduced the systematic error for the binding energy extraction and yielded a more accurate absolute calibration of the magnetic spectrometers.

## 2 Improved experimental setup of the 2014 beam-time

The experimental setup is shown in Fig. 1. Kaons from the strangeness production reaction off the  ${}^9\text{Be}$  target were tagged in forward direction by the KAos spectrometer. Two different target thicknesses of 23 and 47 mg/cm<sup>2</sup> were used. The  ${}^4_{\Lambda}\text{H}$  hypernuclei were formed as hyperfragments and the  $\pi^-$  from the two-body decay  ${}^4_{\Lambda}\text{H} \rightarrow {}^4\text{He} + \pi^-$  at rest were observed. The  $\pi^-$  momentum spectra were measured with two spectrometers SpekA and SpekC, described in Ref. [7]. In order to check systematic momentum uncertainties the acceptance of two spectrometers covered the  ${}^4_{\Lambda}\text{H}$  decay-momentum region simultaneously. The use of large solid angle spectrometers and good background rejection techniques are crucial ingredients for this experiment. Accidental background was reduced by heavier shielding of the photon beam-dump and stronger positron absorption in the KAos spectrometer.

Energy-loss fluctuations in the scattering chamber windows could be eliminated in the 2014 beam-time by directly coupling the vacuum system of the spectrometers to the chamber. Two tungsten alloy collimators were placed behind the target to reduce the coincident background from quasi-free produced  $\Sigma^-$  decays in flight. The collimator blocks had thicknesses of 30 mm and their positions as shown in Fig. 1 (right) were optimized to stop low-momentum decay-pions originating from a decay-region a few cm behind the target.

The magnetic fields of the spectrometers were monitored continuously throughout the beam-time with NMR measurements every 5 minutes. Variations of the magnetic fields of the spectrometers corresponded to less than  $\delta p_{\text{stabil.}} < 4$  keV/c as compared to 40 keV/c in 2012.

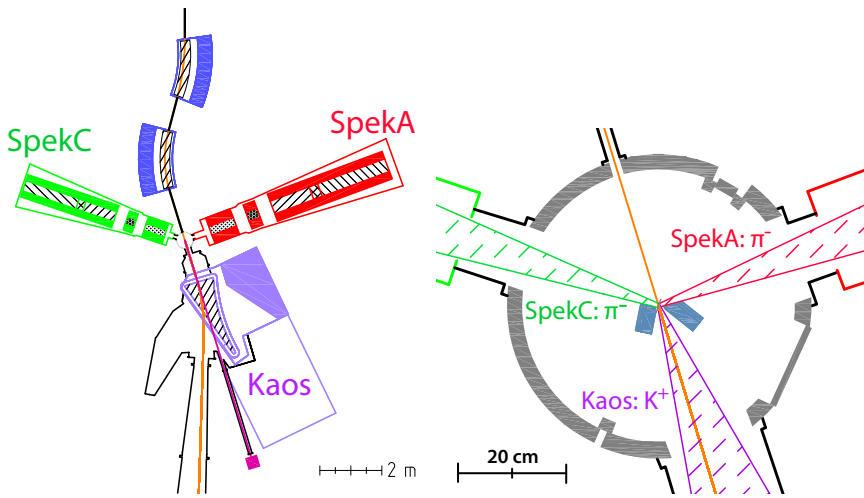


**Figure 1.** Left: Setup of electron beam-line and magnetic spectrometers in the experimental hall at the Mainz Microtron MAMI. The beam entered from top and was deflected by a magnetic chicane before hitting the target with an angle of  $17^\circ$  with respect to the incoming direction. About 1 m downstream of the target the beam was deflected by the K $\alpha$ os spectrometer. Photons from Bremsstrahlung reactions in the target were stopped in a separate beam-dump. Right: Enlarged view of the target region showing the position of the tungsten alloy collimators. All spectrometers, the scattering chamber, and the beam-line formed a common vacuum system.

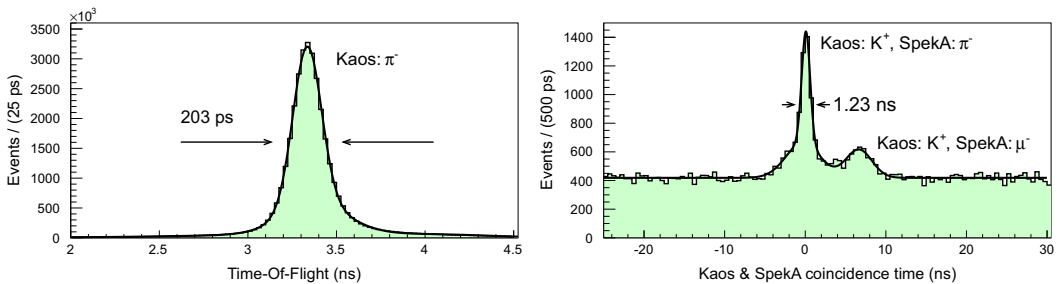


**Figure 2.** Left: Measured time-of-flight for pions inside the K $\alpha$ os spectrometer along a normalized flight path length of 1 m. Right: Coincidence time distribution for kaons in the K $\alpha$ os spectrometer and pions and muons in SpekA. The background includes mis-identified particles near to the central peak and a flat distribution of accidental coincidences.

### 3 Improved calibrations of the 2014 beam-time

#### 3.1 TOF detector calibrations

For the identification of decay-pions it is crucial to have an efficient kaon tagging in combination with a sharp cut on the coincidence time due to the huge background of pions and protons at very forward angles. The coincidence requirement improves dramatically the signal-to-noise ratio but places stringent requirements on the calibration of the time-of-flight (TOF) detectors in the K $\alpha$ os spectrometer. In particular, any changes of ambient parameters like temperature, beam intensity, or

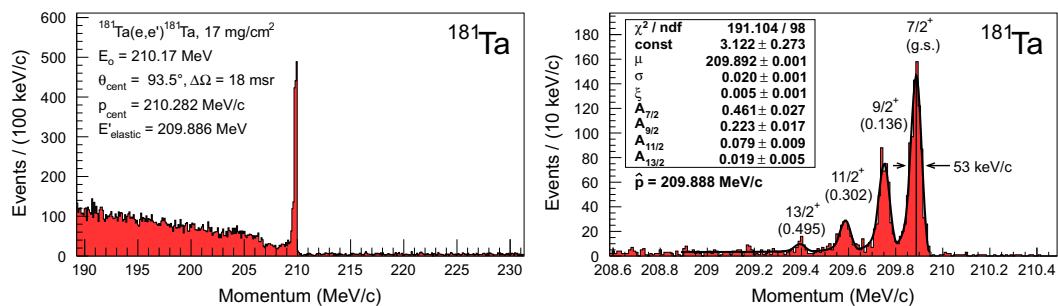


**Figure 3.** Left: Measured momentum spectrum for the  $^{181}\text{Ta}(e, e')^{181}\text{Ta}$  reaction. Target thickness, reaction kinematics, spectrometer settings, and calculated energy for elastic scattering are given. Right: Fit of the peak region in the momentum spectrum with a sum of four Landau distributions convoluted with a Gaussian resolution function on top of a constant background. Three low-lying excited states were resolved and characterized by  $J^P$  quantum numbers and excitation energy. The ground-state FWHM of 52 keV/c and the peak maximum position  $\hat{p}$  are indicated.

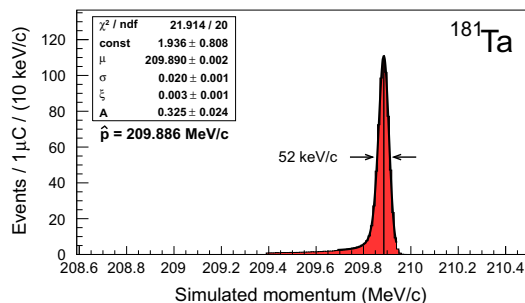


**Figure 4.** Simulated momentum spectrum for the elastic scattering reaction  $^{181}\text{Ta}(e, e')^{181}\text{Ta}$  in the same kinematics as the measurements shown in Fig 3. The peak was fitted with a Landau distribution convoluted with a Gaussian resolution function. The FWHM of 52 keV/c and the peak maximum position  $\hat{p}$  are indicated.

background particle flux could lead to a reduction in kaon tagging efficiency. For the 2014 beam-time an automatic correction was employed for every control setting of all 60 TOF detector segments for every one of the 1201 data runs. In total, more than 370 000 parameter values were calculated and used for the hypernuclei analysis. Fig. 2 shows the measured time-of-flight for pions inside the KAOS spectrometer after calibration. The FWHM  $\approx 200$  ps is a factor of 2 better than in the 2012 beam-time. This high resolution for the TOF measurement is also reflected in a better resolved coincidence time. Further improvements have been achieved for the measurement of the particle's energy-loss and Cerenkov light yield.

### 3.2 Absolute momentum calibration

Detailed measurements with electron beams of energies 195 and 210 MeV have been performed for an absolute momentum calibration and to study the properties of the two spectrometers SpekA and SpekC. As targets, a  $^{181}\text{Ta}$  target of 6  $\mu\text{m}$  foil thickness, corresponding to 10 mg/cm<sup>2</sup> mass thickness, and a  $^{12}\text{C}$  target of 450  $\mu\text{m}$  foil thickness, corresponding to 100 mg/cm<sup>2</sup> mass thickness, were used. Due to tantalum's large mass it experiences relatively little recoil compared to carbon, making it an excellent choice for calibration. The target foils were tilted by 54 $^\circ$  with respect to the incoming beam.

The beam energy was measured in the third stage of the racetrack microtron cascade with an absolute accuracy of  $\delta E_{beam} = \pm 160$  keV by exact determination of the beam position on the accelerator axis and in a higher return path.

As a result, Fig. 3 shows a momentum spectrum of electrons scattered on  $^{181}\text{Ta}$  at a scattering angle of  $93.5^\circ$ , corrected for kinematic broadening. Three low-lying rotational states were clearly resolved. The spectrum was measured with SpekA using a solid angle of 18 msr. As compared to the full value of 28 msr the acceptance angle cuts reduced the aberration effects slightly. The elastic line for the reduced acceptance had a width of 53 keV/c (FWHM), corresponding to a momentum resolution of  $\delta p/p \approx 2 \times 10^{-4}$ . The width increased by 10 keV/c for the full solid angle.

The ground-state line was fitted with a Gaussian distribution corresponding to the spectrometer resolution  $\mathcal{G}(p, \mu, \sigma)$  parameterized with the expectation value  $\mu$  and variance  $\sigma^2$ . This distribution was folded with the energy-loss distribution represented by a numerical approximation of the Landau distribution  $\mathcal{L}(p, p_0, \xi)$  with  $\xi$  quantifying the width of the distribution and a shift between the most probable value  $p_0 = \mu + 0,22278298 \xi$  and the position  $\mu$ . The spectrometer response function used for the fitting of the calibration data is then  $\mathcal{A}(p, \mu, \sigma, \xi, A) = A \cdot (\mathcal{G} * \mathcal{L})(p)$ .

Several calibration measurements for different momentum settings were taken. For the computation of new spectrometer calibration values only tantalum elastic scattering data were employed. The calibration was fixed at the relative momentum closest to where the decay-pion line of  $^4_\Lambda\text{H}$  was observed. The data shown in the figure was taken at a 7 % shifted momentum setting. The difference between the calculated elastic line position  $E'_{elastic}$  after energy-loss corrections and the observed line position was of the order of 2 keV/c.

For the determination of the energy-loss entering the calibration the spectra were simulated with a Monte Carlo code taking into account the energy-loss of the incoming beam in the target, the reaction vertex distribution inside the foil, the reaction kinematics, and the energy-loss of the outgoing electron in the target and the spectrometer exit foils. The simulation included ionization losses according to Landau's theory for thin absorbers and internal and external radiation losses. Fig. 4 shows the simulated elastic line for the same kinematics as the measurements shown in Fig. 3 using the design values for the momentum resolution. The shape and width of the line were reproduced.

The excitation spectrum of the  $^{12}\text{C}(e, e')^{12}\text{C}$  reaction was used to check the linearity of the momentum scale. Fig. 5 (left) shows the excitation spectrum of carbon for one spectrometer setting. The expected positions of eight identified states, calculated from the known excitation energies, were indicated by arrows. Several of these states could be fitted for the same setting, in total 21 fits were performed. As an example the fit to the  $J^P = 2^+$  state for this setting is shown in Fig. 5 (right). The carbon lines are wider than the tantalum lines because of the larger energy-loss straggling in the target. From the observed aberration effects along the full momentum acceptance differences of the order of 20 keV/c between the setting shown in Fig. 3 and the calibration point were observed.

In summary, the energy-loss calculation, fit procedure, remaining aberration effects, and the limited statistics can add up to a systematic error of 10 keV/c. Fluctuations in the magnetic field could lead to errors not larger than 5 keV/c. The whole calibration procedure was also applied to SpekC.

## 4 Discussion

A preliminary analysis of these data confirmed in both spectrometers the mono-energetic line from pionic  $^4_\Lambda\text{H}$  decays stopped in Be targets of two different thicknesses. In comparison to the 2012 beam-time the 2014 beam-time profited from improved calibrations which reduced the systematic error on the extraction of the  $^4_\Lambda\text{H}$  binding energy. The remaining systematic error of the binding energy originating from the calibration procedure is  $< 5$  keV for SpekA and  $< 20$  keV for SpekC while the

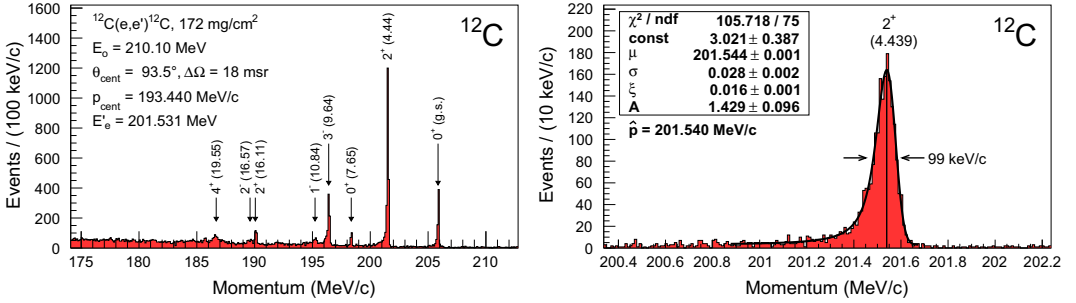


**Figure 5.** Left: Measured momentum spectrum for the  $^{12}\text{C}(e,e')^{12}\text{C}$  reaction. Several excited states over the full momentum acceptance were resolved and characterized by  $J^P$  quantum numbers and excitation energy. Target thickness, reaction kinematics, spectrometer settings, and calculated scattering energy for excitation of the first  $J^P = 2^+$  state are given. Right: Fit of the peak region for this state with a Landau distribution convoluted with a Gaussian resolution function on top of a constant background. The FWHM of 99 keV/c and the peak maximum position  $\hat{p}$  are indicated.

dominant source of systematic uncertainty of 70 – 80 keV originates from the absolute accuracy of the beam energy measurement. The control and stability of the magnetic fields contributes < 5 keV compared to  $\sim 30$  keV in 2012. Measured values of the binding energy with the two spectrometers and the two different target thicknesses will be published in a forthcoming publication.

The calibrations were performed so that future improvements in the beam energy measurements could be used to correct a posteriori the uncertainties of the MAMI 2014 beam-time results. The correction will affect only the central momenta of the spectrometers. A typical energy spread of the extracted MAMI beam is 13 keV with the absolute energy known with an accuracy of  $\delta E_{\text{beam}} \approx \pm 160$  keV. To establish a factor 10 improvement in precision a dipole magnet will be used as a beam-line spectrometer. This method requires the measurement of its field map with a precision in the range of  $\mu\text{T}$  and a stability of the setup on the level of  $20 \mu\text{m}$  over an area of  $5 \times 2 \text{ m}^2$ .

## Acknowledgements

This work was supported in part by Deutsche Forschungsgemeinschaft (SFB 1044), the Carl Zeiss Foundation, European Community Research Infrastructure Integrating Activity FP7, U.S.-DOE Contract No. DEFG02-97ER41047, the Strategic Young Researchers Overseas Visits Program for Accelerating Brain Circulation (R2201), and the Core-to-Core program (21002) of JSPS.

## References

- [1] A. Esser et al. (A1 Collaboration), Phys. Rev. Lett. **114**, 232501 (2015)
- [2] M. Jurić et al., Nucl. Phys. B **52**, 1 (1973)
- [3] G. Bohm et al., Nucl. Phys. B **4**, 511 (1968)
- [4] W. Gajewski et al., Nucl. Phys. B **1**, 105 (1967)
- [5] D.H. Davis, Nucl. Phys. A **547**, 369 (1992)
- [6] A. Gal, Phys. Lett. B **744**, 352 (2015)
- [7] K.I. Blomqvist et al. (A1 Collaboration), Nucl. Instrum. Meth. Phys. Res. A **403**, 263 (1998)